DIY image analytics for UAS-based plant phenotyping

James Kim[1]

[1]Affiliation not available

October 30, 2023

Abstract

UAS-based image analytics has been deployed to expedite the plant phenotyping and replace laborious manual notetaking but is limited for global validation in all field conditions. Plot-level metrics is essential for plant phenotyping on many plots and extracted by defining a region of interest (ROI) of the field boundary and processing sub-ROIs aligned with rows and columns of the total number of plots, called gridding. Gridding is offered by commercial software but is limited to upright rectangular fields. When UAS tile images are stitched, an orthomosaic image is georeferenced to make the image top to north, whereas the field orientation is often off the north. Due to the misaligned orientation, the gridding process requires a preprocess of image rotation to align the grid onto the field boundary, which creates resampling errors and takes laborious multiple adjustments to precisely align sub-ROIs with plots across the field. To address this issue, an open-source software was developed to generalize the gridding method and provide a quick extraction of plot-level metrics without the image rotation. Adaptive gridding algorithm is to rotate the grid by applying geometry of a rectangle in a circle that keeps right angles. Metrics of the rotated ROI is calculated by geofencing pixels in the ROI for segmentation, filtering, masking, and clustering. The open-source software with adaptive gridding allows the end-users to process their UAS images for high throughput phenotyping in an effective manner without understanding details of image processing.

James Y. Kim

USDA-ARS Sugarbeet and Potato Research Unit, Fargo, ND, USA

ORCiD: 0000-0003-0902-065X

Keywords: plant phenotyping, UAS, image analytics, gridding, open-source software, Python.

INTRODUCTION

Plant phenotyping is a vital practice in plant breeding and biotechnology to discover a new variety or characterize desired genetic traits resistant to biotic and abiotic stresses. High throughput phenotyping (HTP) is essential to meet the timely delivery of the phenotypic metrics of a large number of plots. Conventional phenotyping is made by notetaking to score the plant health conditions, which is laborious and inconsistent. Image-based HTP was deployed to replace manual scoring and achieve the rapid extraction of phenotypic metrics using ground and aerial platforms. Plot-level metrics is required for plant phenotyping on a large number of plots and extracted by defining a region of interest (ROI) of the field boundary and processing sub-ROIs aligned with rows and columns of the total number of plots, called gridding. Grid-based image processing is offered by commercial software (e.g., ArcGIS) but is limited to upright rectangular fields and manual drawing of polygons.

Unmanned aircraft system (UAS) has been widely used to deliver a massive volume of images in high resolution and extract metrics by examining spectral signature and morphological features of the plants. Raw UAS images are preprocessed for orthomosaicing through global positioning system (GPS) and inertial measurement unit (IMU) information using commercial software (e.g., Pix4Dmapper, Agisoft). The orthomosaiced image is georeferenced to align the image top to north, whereas the field orientation is often off the north, resulted by various field layout and declination of magnetic north (used by IMU) from geographic north up to 20 degrees [1]. In practice, no fields are truly oriented to north. This misalignment of the field orientations occurs to any airborne images not only from UASs but also from manned airplanes or satellites, as their image products are all georeferenced. Due to the misaligned orientation, gridding requires a preprocess of image rotation to make the field orientation upright to be aligned with the grid [2], because the computation pattern is sequenced by row (i) and column (j) in image coordinates and performs metrics extraction based on upright rectangular ROIs. Finding a rotation degree, however, takes multiple adjustments to precisely align sub-ROIs with plots across the field, which is a laborious time-consuming task and leads to a heavy computational load especially on the big-sized (e.g., >1 GB) orthomosaic image. Image rotation also creates resampling errors due to the changes of pixel values in repositioned geometry. To solve this issue, gridding method must be generalized for the various field orientations and sizes without changing the original image. The grid rotation and metrics extraction on the rotated sub-ROIs are key challenges in image processing.

This adaptive gridding method will help creating a GIS interface of the grid by converting sub-ROIs to a shapefile that contains a list of plot polygons with GPS coordinates.

The objective of the study is to develop open-source software that provides a quick extraction of plot-level metrics of the field image without the image rotation. Specific objectives are to 1) develop algorithm to create a rotated grid that fits the field and plot boundaries aligned with all sub-ROIs, 2) to extract metrics on the rotated ROIs by geofencing algorithm, 3) publish the software available to the public that automates the adaptive gridding process in graphic user interface (GUI).

MATERIALS AND METHODS

UAS images are collected for field mapping and registered with GPS coordinates and IMU data based on flight waypoints and signal communication (Fig. 1). The UAS receives GPS signals from satellites and correction signals from a real-time kinematic (RTK) base station or NTRIP (Networked Transport of RTCM via Internet Protocol) service. The raw UAS images are preprocessed for stitching tile images to an orthomosaic image in field level.

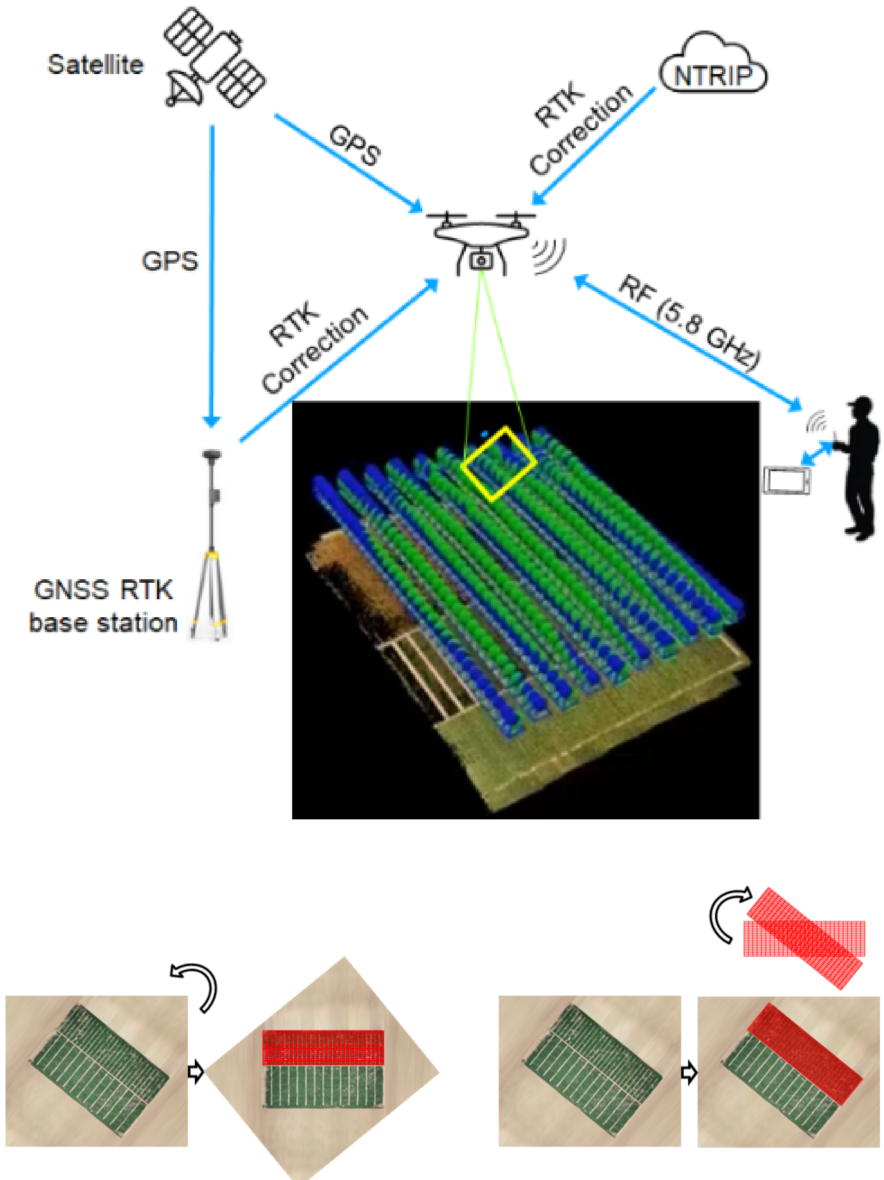

(a) (b) (c)

Figure 1. Schematic of UAS imaging and processing: (a) setup for field mapping based on flight waypoints and signal communication, (b) conventional gridding by image rotation, and (c) adaptive gridding by grid rotation.

The orthomosaic image is processed for plot-level metrics extraction on a large number of plots by defining a grid that is spaced by rows and columns of the total number of plots and by processing sub-ROIs in the grid. Conventional gridding offered by commercial software (e.g., FIELDimageR) requires image rotation to achieve an upright rectangular field so that the grid is aligned with the field and computed by row (i) and column (j) of image coordinates (Fig. 2a). Adaptive gridding algorithm is to eliminate the image rotation and instead simply rotate the grid (Fig. 2b) that is aligned with the rotated field and extract metrics from the rotated sub-ROIs.

2.1 Grid rotation

A rotated grid is drawn by rotating an outer ROI over the field boundary and adding internal horizontal and vertical lines at the rotation angle within the outer ROI. The grid rotation is implemented by applying a geometric property of a rectangle in a circle that keeps right angles at four corners when the inner rectangle is rotated and reshaped within a circle by pivoting two diagonal corners. When two diagonal corners A (i_1, j_1) and C (i_2, j_2) are known, therefore, the other two diagonal corners B (i_3, j_3) and D (i_4, j_4) are uniquely defined with an arbitrary i along the circumference (Fig. 2a) by using Eqs. (1) and (2).

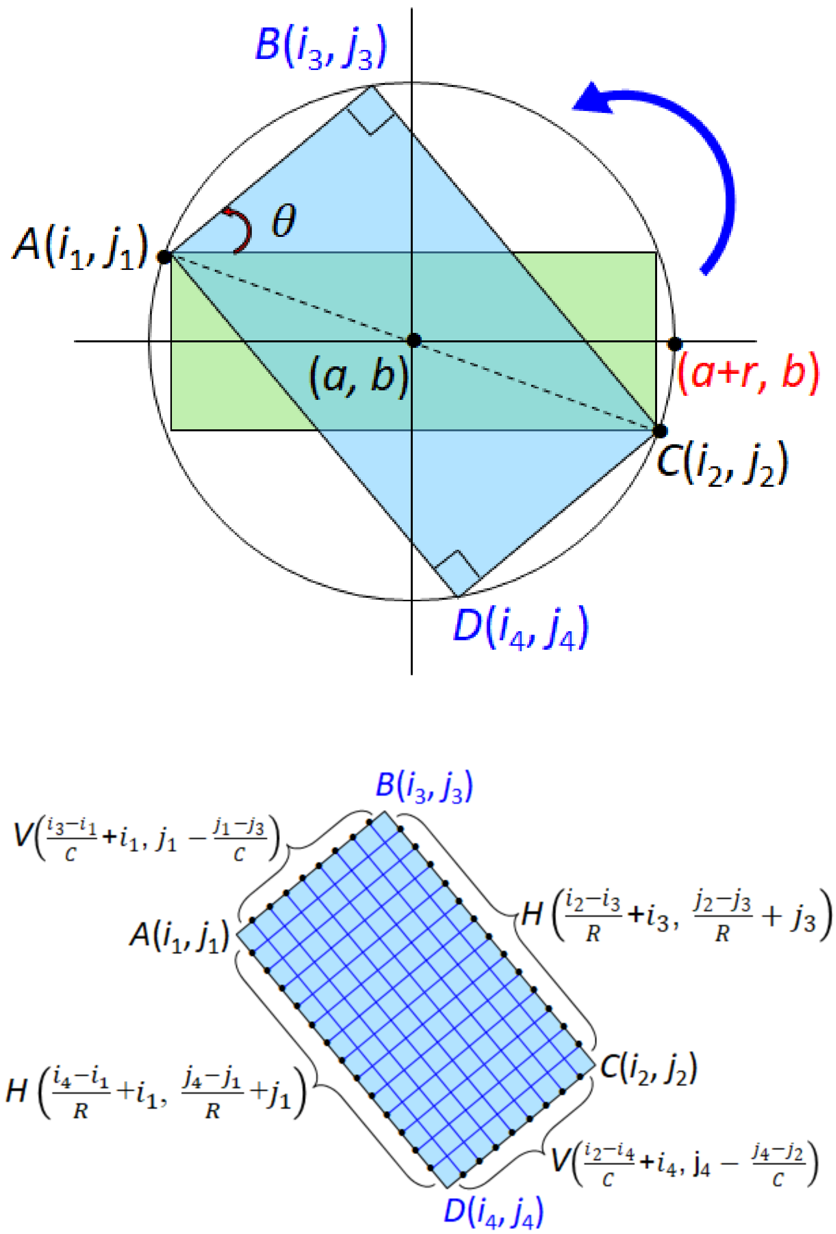

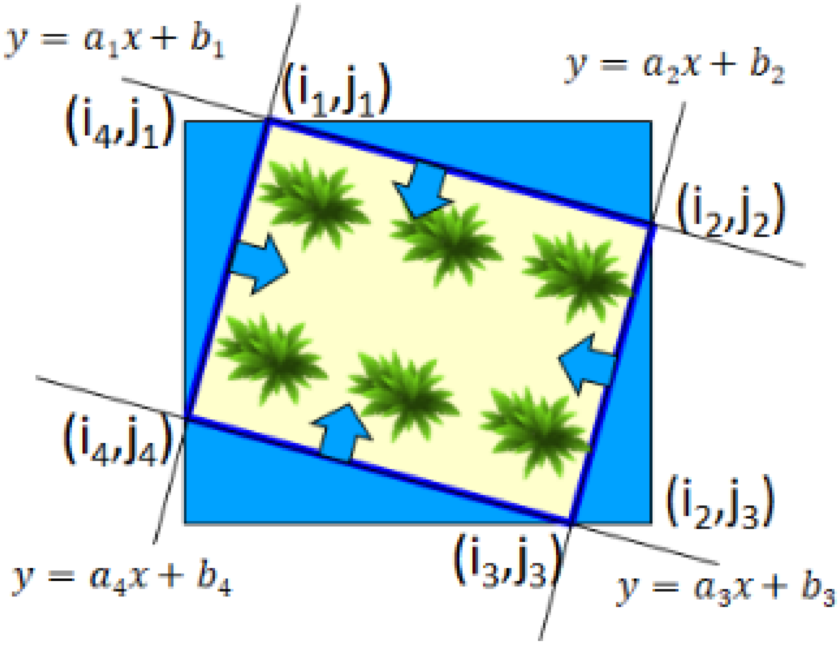
$y = a_1x + b_1$
(i_1,j_1)
$y = a_2x + b_2$
(i_4,j_1)
(i_2,j_2)
(i_4,j_4)
(i_2,j_3)
(i_3,j_3)
$y = a_4x + b_4$
$y = a_3x + b_3$

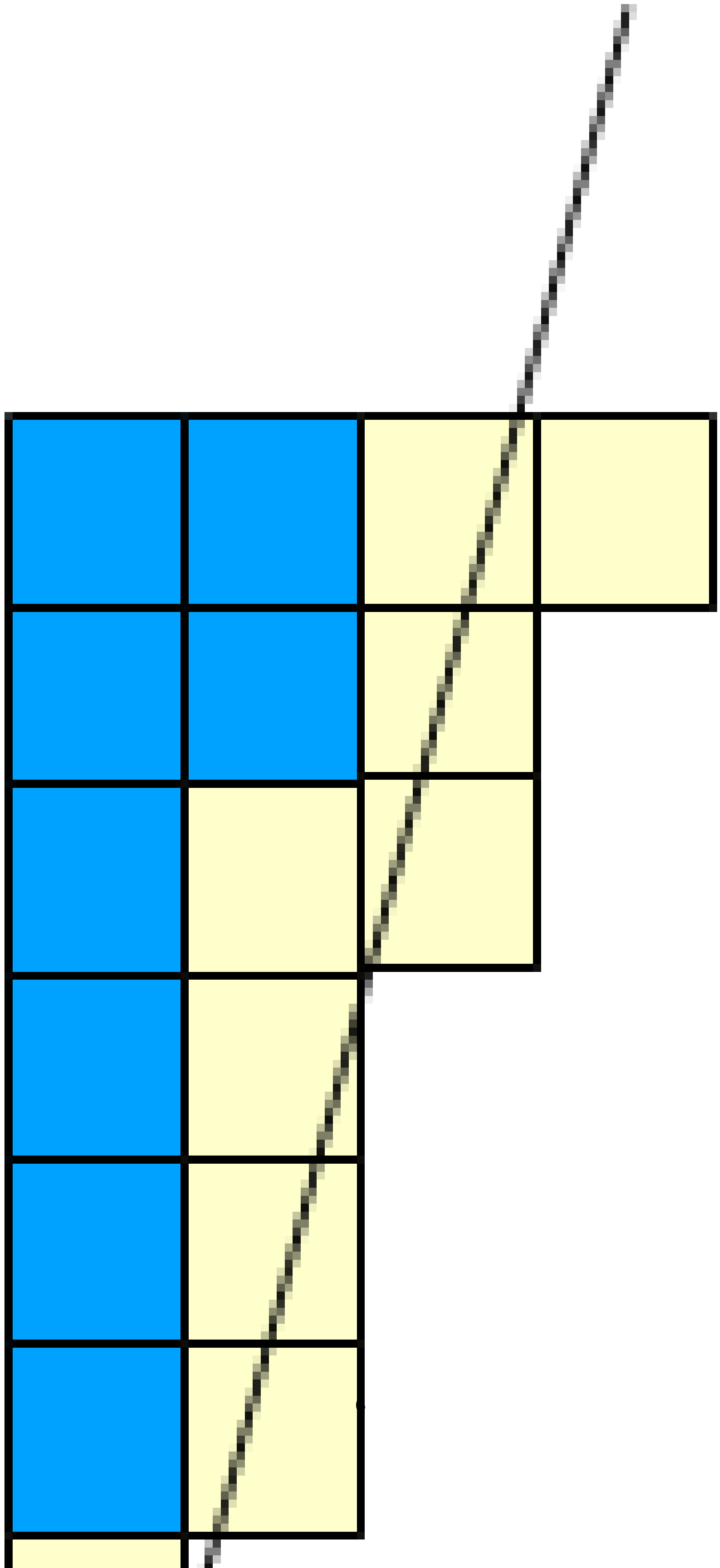

(a) (b) (c) (d)

Figure 2. Grid rotation and metrics extraction from the rotated ROI: (a) geometry of a rectangle in a circle that keeps right angles at four corners when the inner rectangle is rotated and reshaped within a circle by pivoting two diagonal corners A and B, (b) a rotated grid drawn by connecting two edge points along the horizonal (H) and vertical (V) directions created by the number of rows (R) and columns (C), (c) geometry of the rotated ROI, and (d) geofencing of the rotated ROI to locate pixels only inside the ROI for metrics extractions.

$B\left(i_3, j_3\right) = (i, \pm\sqrt{r^2 - (i-a)^2} + b)(1)$

$D\left(i_4, j_4\right) = \left(a + \left(a - i_3\right),\ b + \left(b - j_3\right)\right)(2)$

where r is a radius and the center (a, b) of the rectangle is defined by

$a = \frac{i_2 - i_1}{2} + i_1, b = \frac{j_2 - j_1}{2} + j_1$ (3)

and the circle is formulated in i -j image coordinate system in Eq. (4).

$j = \pm\sqrt{r^2 - (i-a)^2} + b$ (4)

When all four corners of a rotated rectangular ROI are calculated by Eqs. (1) and (2), a rotated grid is drawn by connecting two edge points along the horizonal (H) and vertical (V) directions (Fig 2b) created by the number of rows (R) and columns (C) as shown in Eqs. (5) and (6).

$H = \left[\left(\frac{i_4 - i_1}{R} + i_1,\ \frac{j_4 - j_1}{R} + j_1\right), \left(\frac{i_2 - i_3}{R} + i_3,\ \frac{j_2 - j_3}{R} + j_3\right)\right](5)$

$V = \left[\left(\frac{i_3 - i_1}{C} + i_1,\ j_1 - \frac{j_1 - j_3}{C}\right), \left(\frac{i_2 - i_4}{C} + i_4,\ \mathrm{j4} - \frac{j_4 - j_2}{C}\right)\right](6)$

To visualize the grid rotation in GUI, the grid is validated in a full range of the rotation angle (ϑ) until the maximum angle ($\vartheta_{\mu\alpha\xi}$) calculated by

$\theta = \left(\frac{j_3 - j_1}{i_3 - i_1}\right), \theta_{\max} = 90 + \theta\mathrm{min}$ (7)

In completing the full range of the grid rotation, when the rotation brings the corner B (i_3,j_3) crossed at ($a + r$, b), i.e., at a crossing angle (ϑ_{cross}) (Eq. 8), the sign of $\sqrt{r^2 - (i-a)^2}$ inj_3 must be reversed due to the change of the direction from b in j -coordinate (Fig. 2a). This critical point is detected by formulating i_3 using Eq. (10) from the interaction of a circle (Eq. 6) and a line (Eq. 9).

$\theta_{\text{cross}} = \left(\frac{a + r - i_1}{b - j_1}\right)(8)$

$j = s * i + \left(j_1 - s * i_1\right)$ (9)

$i_3 = \left[-(2K * s - 2a) + sqrt\left(-(2K * s - 2a)^2 + 4(s^2 + 1)(K^2 - r^2 + a^2)\right)\right] / 2(s^2 + 1)(10)$

where s is a slop that is calculated by tan (ϑ) and$K$ is

$K = \left(j_1 - s * i_1\right) - b$ (11)

2.2 Metrics from rotated ROI

Metrics of the rotated grid is calculated by geofencing pixels within the rotated sub-ROIs for segmentation, filtering, masking, and clustering. Figure 3 illustrates how the rotated ROI is positioned and geofenced to process only pixels inside the ROI for metrics extractions. When the grid is rotated, each rotated sub-ROI is defined with four corners (i_1, j_1), (i_2, j_2), (i_3, j_3), and (i_4, j_4) that are intersections of the four rotated edge lines, whereas an outer upright rectangle is formed by (i_4,j_1), (i_2,j_1), (i_2,j_3), and (i_4,j_3) (Fig. 2c). Geofencing is to register pixels within the inner rotated ROI among all pixels in the outer rectangle. The slop (a_1) and j -intercept (b_1) of the first edge line ($j = a_1 i + b_1$) are calculated from (i_1, j_1), (i_2, j_2) by (j_2-j_1)/(i_2 -i_1) and (j_1-$a_1 i$), respectively. When all four edge lines are similarly formulated, each pixel is compared with four lines and selected if j -coordinate falls within four lines. When i is plugged into the line equations, four j -values on the lines are calculated. The pixel (i, j) is selected as an ROI pixel, if j falls within four j -values ranged by a minimum and a maximum in each of vertical (min_V, max_V) and horizontal (min_H, max_H) directions (Eqs. 15 and 16).

$$min_V, max_V = \min(a_1 * i + b_1, a_3 * i + b_3), \max(a_1 * i + b_1, a_3 * i + b_3) \quad (15)$$

$$min_H, max_H = \min(a_2 * i + b_2, a_4 * i + b_4), \max(a_2 * i + b_2, a_4 * i + b_4) \quad (16)$$

Assuming an origin at the left top corner, for instance, when i -coordinate 1 of pixel at (1, 0) is tested with the lines, fourth j -value $a_4 + b_4$ becomes a minimum in the vertical direction which is greater than j -coordinate 0 and makes the pixel beyond the ROI, whereas when i -coordinate 2 of pixel at (2, 2) is tested with the lines, fourth j -value $2a_4 + b_4$ as a minimum is equal to j -coordinate 2 and thus makes the pixel in the ROI (Fig. 2d).

RESULTS AND DISCUSSION

The algorithm was tested on a sample field image that contains a field orientation misaligned with north. Open-source software, image mapping and analytics for phenotyping (IMAP) [3], was successfully upgraded with adaptive gridding method. Figure 3a illustrates a screenshot of the IMAP software that demonstrates a rotated grid (10×28) in a circle and a vegetation segmentation within the grid of 10 rows and 28 columns. Phenotypic metrics of total 280 plots is exported to a csv file (Fig. 3b) and plotted in a graph (Fig. 3c).

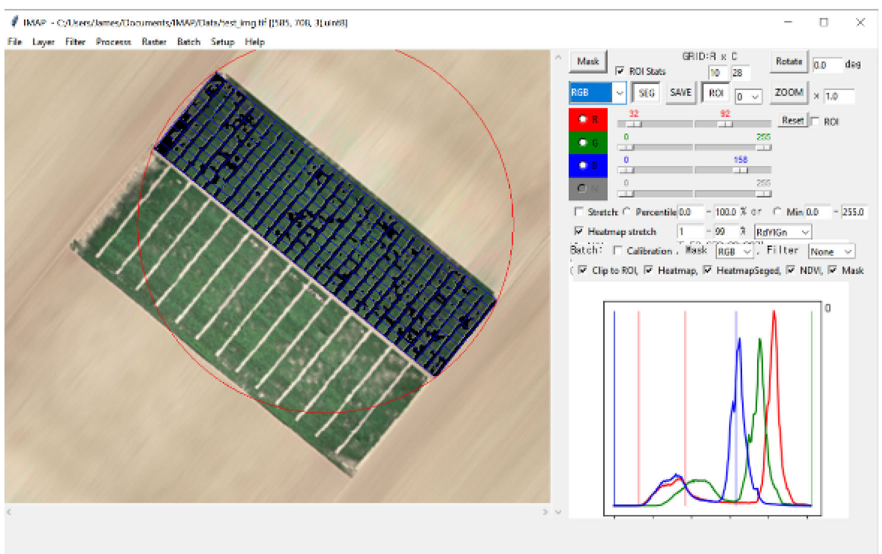

Iter	Row	Col	cnt_Fgnd	cnt_ROI	%Canopy	R [%]	G [%]	B [%]	H	S	V	NDVI
1	1	1	42	208	20.19	32.31	34	27.37	53.45	50	86.81	0.5345
2	1	2	132	207	63.77	30.13	33.73	26.12	62.06	58.63	86.03	0.6206
3	1	3	118	219	53.88	27.96	32.09	24.66	65.9	59.86	81.82	0.659
4	1	4	172	210	81.9	25.04	30.21	22.73	72.35	63.9	77.04	0.7235
5	1	5	177	218	81.19	21.44	28.27	20.21	78.83	74.24	72.09	0.7883
6	1	6	187	210	89.05	19.75	29.47	19.58	84.23	89.91	75.14	0.8423
7	1	7	191	218	87.61	18.84	30.3	19.28	86.72	100.37	77.27	0.8672

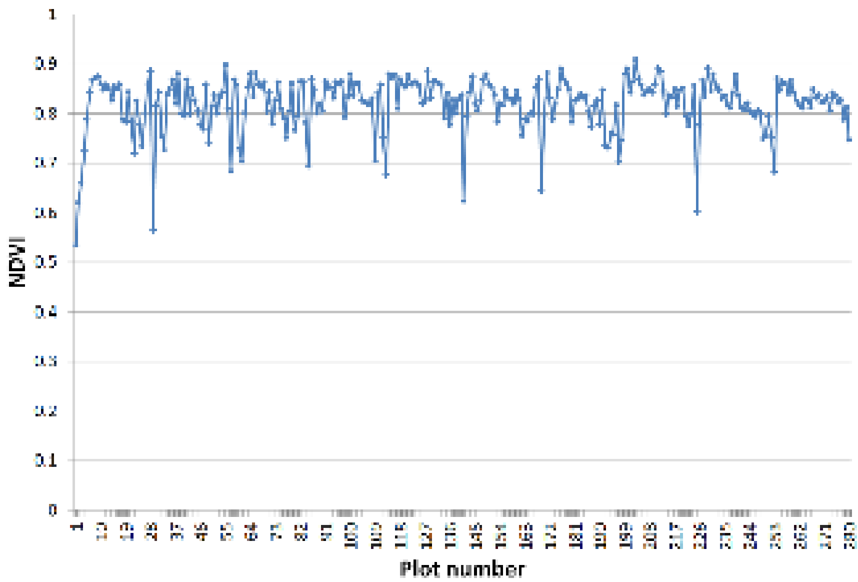

(a) (b) (c)

Figure 3. Experiment on a sample image: (a) a screenshot of the open-source software IMAP that demonstrates vegetation segmentation in a rotated grid, (b) output metrics exported to a csv file, (c) a graph displaying metrics of 280 plots.

CONCLUSIONS

Adaptive griding algorithm was developed and successfully implemented on a sample field image by using geometry of a rectangle in a circle. Plot-level metrics was extracted by georeferencing pixels only within a ROI. Grid rotation and metrics extraction were interfaced graphically for user-friendly operations. The open-source software with adaptive gridding is publicly available [4] and allows the end-users to process their UAS images for high throughput phenotyping in an effective manner without knowledge of image processing. This new gridding method can be also extended to other types of images from ground and satellite platforms that contain multiple plots in various orientations.

ACKNOWLEDGMENTS

This research was funded by the U.S. Department of Agriculture, Agricultural Research Service under project numbers 6066-13000-005-00D and 3060-21000-044-00D.

REFERENCES

[1] USGS, “Magnetic declination varies considerably across the United States”, Educational Resources, <https://www.usgs.gov/educational-resources/magnetic-declination-varies-considerably-across-united-states> (26 October 2023).

[2] FIELDimageR, “A Tool to Analyze Images From Agricultural Field Trials and Lab in R”, <https://rdrr.io/github/filipematias23/FIELDimageR/f/README.md> (27 October 2023).

[3] Kim, J.Y. “Software design for image mapping and analytics for high throughput phenotyping,” Computers and Electronics in Agriculture 191 (2021) 106550.

[4] Kim. J.Y. “IMAP: image mapping & analytics for phenotyping,” National Agricultural Library. Doi: 10.15482/USDA.ADC/1523140. (2021).